Since January 2020 Elsevier has created a COVID-19 resource centre with free information in English and Mandarin on the novel coronavirus COVID-19. The COVID-19 resource centre is hosted on Elsevier Connect, the company's public news and information website.

Available online at www.sciencedirect.com
SCIENCE DIRECT®
Virology 319 (2004) 249–261
VIROLOGY
www.elsevier.com/locate/yviro

Apoptosis in astrovirus-infected CaCo-2 cells

Susana Guix,[a] Albert Bosch,[a,*] Enric Ribes,[b] L. Dora Martínez,[a] and Rosa M. Pintó[a]

[a] *Enteric Virus Group, Department of Microbiology, University of Barcelona, Spain*
[b] *Enteric Virus Group, Department of Cell Biology, University of Barcelona, Spain*

Received 4 April 2003; returned to author for revision 20 October 2003; accepted 23 October 2003

Abstract

Cell death processes during human astrovirus replication in CaCo-2 cells and their underlying mechanisms were investigated. Morphological and biochemical alterations typical of apoptosis were analyzed in infected cells using a combination of techniques, including DAPI staining, the sub-G_0/G_1 technique and the TUNEL assay. The onset of apoptosis was directly proportional to the virus multiplicity of infection. Transient expression experiments showed a direct link between astrovirus ORF1a encoded proteins and apoptosis induction. A computer analysis of the astrovirus genome revealed the presence of a death domain in the nonstructural protein p38 of unknown function, encoded in ORF1a. Apoptosis inhibition experiments suggested the involvement of caspase 8 in the apoptotic response, and led to a reduction in the infectivity of the virus progeny released to the supernatant. We conclude that apoptotic death of host cells seems necessary for efficient human astrovirus replication and particle maturation.

Keywords: Human astrovirus; Apoptosis; CaCo-2 cells; Caspases; Death domain

Human astroviruses (HAstV) have been increasingly recognized as an important pathogen of acute nonbacterial gastroenteritis in children (Glass et al., 1996). The astrovirus genome consists of a 6.8 kb single-stranded, polyadenylated positive-sense RNA, which is infectious when transfected into permissive cells (Geigenmüller et al., 1997). HAstV can be isolated and propagated in human intestinal CaCo-2 continuous cell line in the presence of trypsin, which is involved in the capsid protein maturation (Monroe et al., 1991).

The organization of the genome includes three ORFs: ORF1a is located at the 5′ end of the genome and contains a serine protease motif, ORF1b contains a RNA-dependent RNA polymerase motif and ORF2 encodes the structural proteins (Matsui and Greenberg, 2001). The nonstructural proteins of the virus are translated from the genomic viral RNA as two polyproteins; one of them contains only ORF1a (101 kDa) and the other includes ORF1a/1b (160 kDa) and is translated via a −1 ribosomal frameshifting event between ORF1a and ORF1b (Jiang et al., 1993). Both proteins are proteolytically processed giving rise to a variety of proteins, although it is not clear whether the viral protease is responsible for all the cleavages (Geigenmüller et al., 2002a, 2002b; Kiang and Matsui, 2002). A subgenomic RNA that contains ORF2 is detected in the cytoplasm of infected cells (Monroe et al., 1991). This subgenomic RNA is translated as a 87-kDa capsid precursor which gives raise to mature capsid proteins in a process that involves trypsin and a putative cellular protease (Bass and Qiu, 2000; Méndez et al., 2002; Monroe et al., 1991) and it has been described by different laboratories that viral particles grown in the absence of trypsin show an importantly reduced infectivity titer (Bass and Qiu, 2000; Méndez et al., 2002; Monroe et al., 1991).

Little is known about human astrovirus pathogenesis. Gray et al. (1980) published some ultrastructural studies on astrovirus-infected lambs, in which they observed astrovirus aggregates within epithelial cell lysosomes and autophagic vacuoles, as well as along microvilli. Macrophages containing virus particles and enterocytes showing microvilli and some nuclear degeneration were also described. Woode et al. (1984) described the degeneration of dome epithelial cells due to astrovirus infection in the ileum of infected

* Corresponding author. Department of Microbiology, School of Biology, University of Barcelona, Avda Diagonal 645, 08028 Barcelona, Spain. Fax: +34-93-4034629.
E-mail address: abosch@ub.edu (A. Bosch).

0042-6822/$ - see front matter © 2004 Published by Elsevier Inc.
doi:10.1016/j.virol.2003.10.036

calves. Recently, a report on the pathogenic effects of poult enteritis and mortality syndrome (PEMS)-turkey astrovirus in macrophages has also been published (Qureshi et al., 2001). Although it was not demonstrated, a relationship between macrophage degeneration and apoptosis may be inferred from this latter work.

Apoptosis is defined as an energy-dependent physiological process of cellular self-destruction in response to a variety of stimuli. It is characterized by a series of morphological changes and biochemical processes including cell shrinkage, chromatin condensation, cleavage of DNA into oligonucleosomal length fragments and, finally, cell fragmentation into apoptotic bodies which are phagocytosed by neighboring cells without causing inflammatory reaction in the tissue (Saraste and Pulkki, 2000). On the one hand, it appears that programmed cell death would serve as a host defense mechanism and obstruct virus replication. On the other hand, in later stages of infection and when enough virus progeny has been generated, apoptosis may also facilitate virus propagation to bystander cells avoiding inflammation. Thus, many viruses including both DNA and RNA viruses have developed strategies either to induce or to inhibit apoptosis at different stages of their replication cycle (Hardwick, 1998; Koyama et al., 2000; Roulston et al., 1999).

The pathways for both induction and prevention of apoptosis are highly complex and still poorly understood. Caspases, a family of cysteine proteases, play a central role in the execution of the apoptotic process (Denecker et al., 2001; Stennicke and Salvesen, 2000). Caspases are synthesized as inactive proenzymes and activated after cleavage at specific aspartate residues in a self-amplifying cascade. Activation of the upstream caspases such as caspases 2, 8, 9, 10 and 12, by pro-apoptotic signals leads to proteolytic activation of the downstream or effector caspases 3, 6 and 7. Two major pathways of caspase activation during apoptosis have been characterized. First, extrinsic activation is driven by activation of caspase 8 and is mainly initiated in response to ligation of cell surface death receptors, which include Fas and TNF receptors. Recruitment of initiator procaspase 8 to activated receptors with involvement of adaptor molecules such as TRADD or FADD, triggers procaspase autoproteolysis by proximity-induced activation. The second apoptotic initiator pathway, intrinsic activation, is initiated by caspase 9 activation after release of cytochrome *c* from the mitochondrial intermembrane space to the cytosol. Cytochrome *c*, together with dATP/ATP binds to Apaf-1, and recruits caspase 9 after a conformational change of Apaf-1. It has recently been observed that some viral mechanisms of either induction or inhibition of apoptosis involve a direct interaction with caspases (Thome et al., 1997). Moreover, some viral proteins have also been described as potential targets for activated caspases (Al-Molawi et al., 2003; Eleouet et al., 2000; Zhirnov et al., 1999).

In the present work, the apoptosis induced in astrovirus-infected CaCo-2 cells is analyzed, and different approaches to study the relationship between apoptosis and the virus life cycle are undertaken.

Results

Apoptosis is induced in astrovirus-infected CaCo-2 cells

To investigate the effect of astrovirus infection on CaCo-2 cells, a set of different techniques was used to analyze most characteristic features of apoptosis. For all the following cellular analysis, CaCo-2 cells were infected with a multiplicity of infection (m.o.i.) of 5 and fixed at different times post-infection (p.i.). Mock-infected cells and aspirin-treated cells were used as negative and positive controls, respectively (see Materials and methods).

Morphological changes in infected CaCo-2 cells were first examined by optical microscopy after DAPI staining. As shown in Fig. 1, nuclear morphological changes could not be observed at 24 h after infection. However, at 48 h p.i., many cells showed a marked condensation of the chromatin and the formation of apoptotic bodies (arrows). In mock-infected cells, the nuclei remained intact and uniformly stained without signs of chromatin condensation even at 48 h p.i.

To quantify the percentage of apoptotic cells, astrovirus-infected and mock-infected cultures were monitored by flow cytometry, employing DNA staining with propidium iodide. During the apoptotic process, the activation of cellular endonucleases results in fragmentation of the nuclear DNA into oligonucleosome-sized fragments, which can be selectively extracted from cells after fixation with ethanol 70% and treatment with phosphate–citrate buffer, resulting

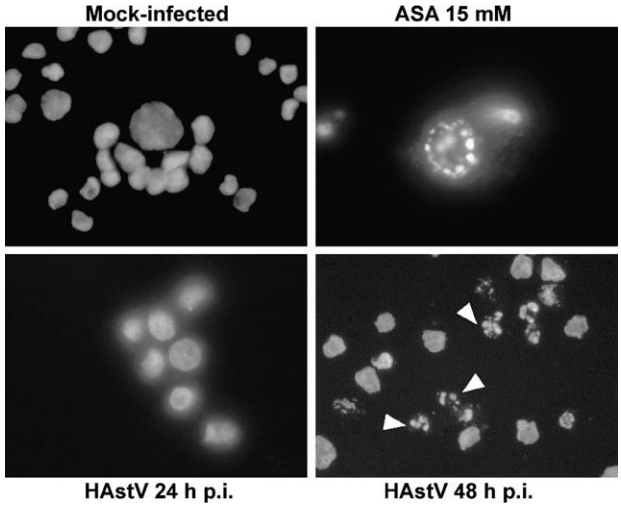

Fig. 1. Morphology of cell nuclei of mock-infected CaCo-2 cells, aspirin-treated cells (ASA 15 mM) and HAstV-infected cells at 24 and 48 h p.i., after DNA staining with DAPI. At 48 h p.i., many infected cells show apoptotic bodies due to the condensation of chromatin in several micronuclei (arrows).

in a reduction of cellular DNA content. The presence of apoptotic cells (sub-G_0/G_1 peak) was detected in DNA content frequency histograms. Aspirin-treated cells exhibited 40.6% of apoptotic cells. In astrovirus-infected cultures, the proportion of apoptotic cells increased from 18.7% at 24 h p.i. up to 27.7% at 48 h p.i., whereas only 6.2% of apoptotic cells were observed in mock-infected cells (Fig. 2).

The TUNEL assay was also performed to further characterize the apoptotic response. The percentage of cells containing DNA strand breaks was quantified by flow cytometry. Using a m.o.i. of 5, astrovirus-infected cells exhibited 70.8% apoptotic cells at 72 h p.i., whereas only 0.2% were observed in mock-infected cultures (Fig. 3A). At 24 h p.i., the percentage of apoptotic cells was only 6.4% (data not shown). In our hands, despite a low degree of variation, percentages of apoptotic cells were generally higher when measured by the TUNEL assay than by the sub-G_0/G_1 technique, indicating that the TUNEL provides a higher sensitivity to detect apoptosis. The TUNEL assay was also used to monitor the onset of apoptosis when using different m.o.i. (5, 0.5 and 0.05). A correlation was observed between the m.o.i. and the percentage of apoptotic cells (Fig. 3B), suggesting a direct relationship between viral infection and apoptosis. In addition, a decrease in the dose of input virus delayed the development of apoptosis. When a m.o.i. of 0.05 was used, a significant proportion of apoptotic cells could not be detected until 96 h p.i.

Finally, ultrastructural modifications in astrovirus-infected cells were examined in detail by transmission electron microscopy at 48 h p.i. (Fig. 4). The formation of masses of condensed chromatin dispersed mostly at the periphery of the convoluted nucleus was observed in infected cells. Other characteristics of apoptosis such as disintegration of nucleoli, while maintenance of intact mitochondria and other cell organelles as well as both

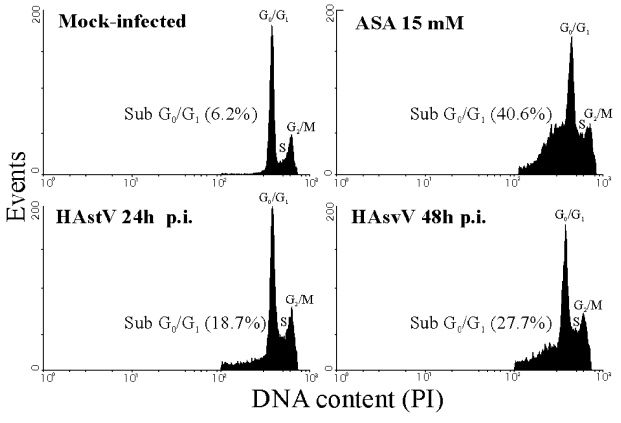

Fig. 2. Flow cytometric analysis of DNA content of propidium iodide (PI)-stained CaCo-2 cells. The percentage of apoptotic cells was obtained by calculating the percentage of the cell population showing a DNA content lower than G_0/G_1 cells in the cell cycle.

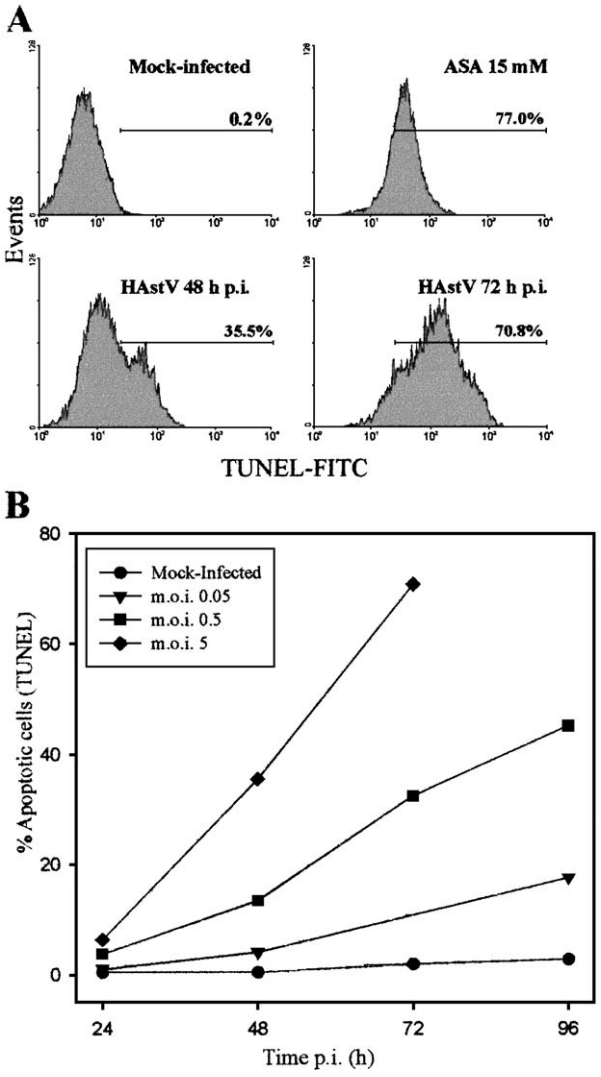

Fig. 3. In situ detection of apoptosis by TUNEL analysis. (A) Flow cytometry analysis of mock-infected cells at 48 h p.i., aspirin-treated cells at 48 h and HAstV-infected cells at 48 and 72 h p.i. after TUNEL staining of apoptotic nuclei. The percentage of apoptotic cells was estimated as the percentage of cells showing FITC fluorescence nuclei, due to the addition of fluorescein dUTP at 3ÓH ends of fragmented DNA. A cursor for FITC positivity was defined from mock-infected cultures, which usually included 0.1–3.0% of the total cell population (in the depicted experiment, it includes only 0.2% of the total population of mock-infected cells). (B) Dose-dependent and time-dependent appearance of apoptotic cells. Cells were infected with different m.o.i., harvested at various times p.i., analyzed by TUNEL assay and subjected to flow cytometry. The values of the error bars, which are not depicted for the sake of clarity, were always below 0.44× the mean value.

nuclear and cytoplasmic membranes were also observed (Figs. 4B and C). On the contrary, control cells exhibited a normal morphology with randomly distributed organelles, a nucleus with finely granular and uniformly dispersed chromatin and a large unique electron-dense nucleolus (Fig. 4A). Astrovirus particles were observed inside most cells that showed these signs of apoptosis (Fig. 4C).

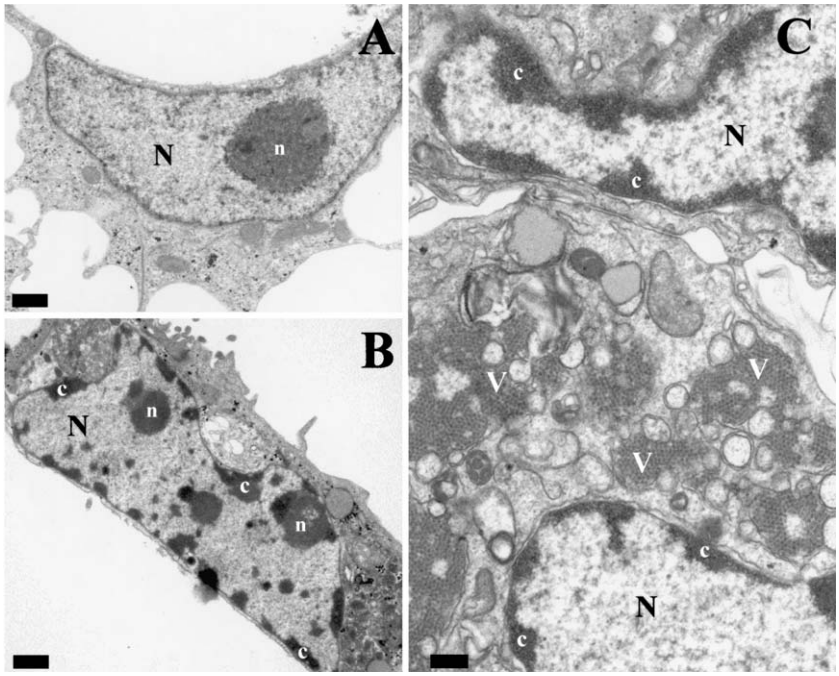

Fig. 4. Electron micrographs of mock-infected (A) and HAstV-infected CaCo-2 cells at 48 h p.i. (B and C). In mock-infected cells, the large nucleus (N) displays a large, unique nucleolus (n). HAstV-infected cells are characterized by numerous masses of condensed chromatin (c) dispersed at the periphery of a convoluted nucleus. Aggregates of astrovirus particles (v) accumulated in the cytoplasm of infected cells (C). Bars equal 1 μm in A and B, and 0.5 μm in C.

In conclusion, the study of nuclear and cellular morphology, the analysis of the reduction of cellular DNA content, and the characterization of DNA fragmentation by TUNEL assay, unambiguously demonstrated that apoptosis is triggered in CaCo-2 cells during astrovirus infection following a dose-dependent pattern.

Caspase 8 is involved in astrovirus-induced apoptosis

With the aim to study the activation of upstream caspases during astrovirus-induced apoptosis, the role of caspase 8 and caspase 9 was analyzed. Caspase 8 was detected by Western blot using a specific antibody with total cell lysates from infected and mock-infected cells harvested at various times p.i. In mock-infected cell lysates, anti-caspase 8 antibody recognized a protein of 55 kDa corresponding to the procaspase form. In addition, a polypeptide of approximately 26 kDa, which corresponds to the prodomain of caspase 8, was also detected in infected cells from 48 h p.i. (Fig. 5A). This result indicates that FLICE/caspase-8 activation takes place during astrovirus infection.

To investigate whether there was also activation of the mitochondrial apoptotic pathway, we analyzed the redistribution of cytochrome *c* from the mitochondrial intermembrane space to the cytosol, as an indication of caspase 9 activation. Fig. 5B shows that at any assayed time after infection, a complete release of cytochrome *c* to the cytosol was never observed and that the amount of cytochrome *c* in the mitochondria did not decrease. The low degree of cytochrome *c* redistribution to the cytosol observed at 48 and 72 h in infected cells could be explained as a result of the amplification of the apoptotic signal which involves

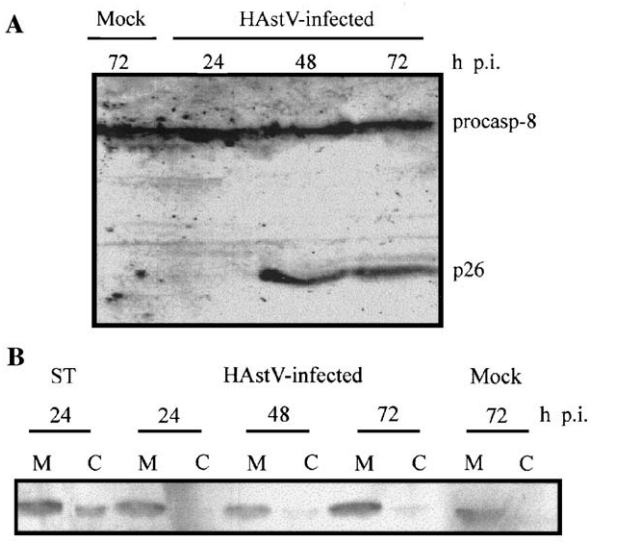

Fig. 5. FLICE/caspase-8 cleavage and distribution of mitochondrial cytochrome *c* during astrovirus infection. (A) Detection of procaspase-8 and activation-resulting product of prodomain p26 by Western blot analysis at the indicated times p.i., according to Medema et al. (1997). (B) Distribution of cytochrome *c* in mitochondrial (M) and cytosolic fractions (C), in 1 μM staurosporine (ST)-treated cells, astrovirus-infected cells at various times p.i. and mock-infected CaCo-2 cells at 72 h p.i.

mitochondrial factors (Denecker et al., 2001; Kidd et al., 2000).

Finally, the role of caspase 8 and 9 in mediating the induction of apoptosis by astrovirus was further assessed by using caspase specific and irreversible peptide inhibitors Z-IETD-FMK (caspase 8) and Z-LEHD-FMK (caspase 9) at different concentrations. The blocking effects of Z-IETD-FMK were dose-dependent (reduction of apoptosis of 7.3% at 10 μM, 23.8% at 100 μM and 39.1% at 150 μM), while Z-LEHD-FMK could inhibit apoptosis only at the highest concentration (reduction of apoptosis of 42.2%). It should be pointed out, however, that the specificity of this compounds when they are used at high concentrations is not always guaranteed (Thornberry et al., 1997). Caspases belonging to Group III (6, 8 and 9) tolerate many different amino acids in P_4 position but prefer those with larger aliphatic side chains. Their optimal peptide recognition motif is (X)E(H/T)D, being all of them quite tolerant to substitutions in P_2. The only exception is caspase 9, which has a stringent specificity for H in P_2 position. Thus, at 150 μM, the blocking effects of Z-LEHD-FMK may be due to a non-specific inhibition of caspase 8, whereas at low concentrations, only the optimal recognition motif may be able to inhibit caspase activation. Consistently, at 10 and 100 μM, only inhibition of caspase 8 had effective effects in reducing the percentage of apoptotic cells after infection, suggesting a relationship between astrovirus infection and caspase 8 activation.

In summary, although caspase 8 inhibitor did not completely block astrovirus-induced apoptosis, these results, together with the analysis of caspase 8 activation by Western blot, provide clear evidence that this caspase is involved in the sequence of events that occur during astrovirus-induced apoptosis.

Viral replication occurs in both apoptotic and non-apoptotic cells; however, infectious progeny is lower when apoptosis is inhibited

The relationship between apoptosis and the virus life cycle was studied by analyzing protein expression in apoptotic and non-apoptotic cell populations and also by analyzing the effect of apoptosis inhibition on virus production.

The kinetics of viral protein expression and the appearance of apoptosis were simultaneously detected by a double-labeling technique. Cells expressing viral capsid proteins were labeled by immunofluorescence using 8E7 monoclonal antibody (Herrmann et al., 1988) and apoptotic nuclei were labeled by using the TUNEL assay. CaCo-2 cells were infected with a m.o.i. of 0.5, to avoid an extensive infection of all the monolayer, and fixed at 20, 48 and 72 h p.i. (Fig. 6). Flow cytometry results indicated that apoptosis was mostly triggered in infected cells and to

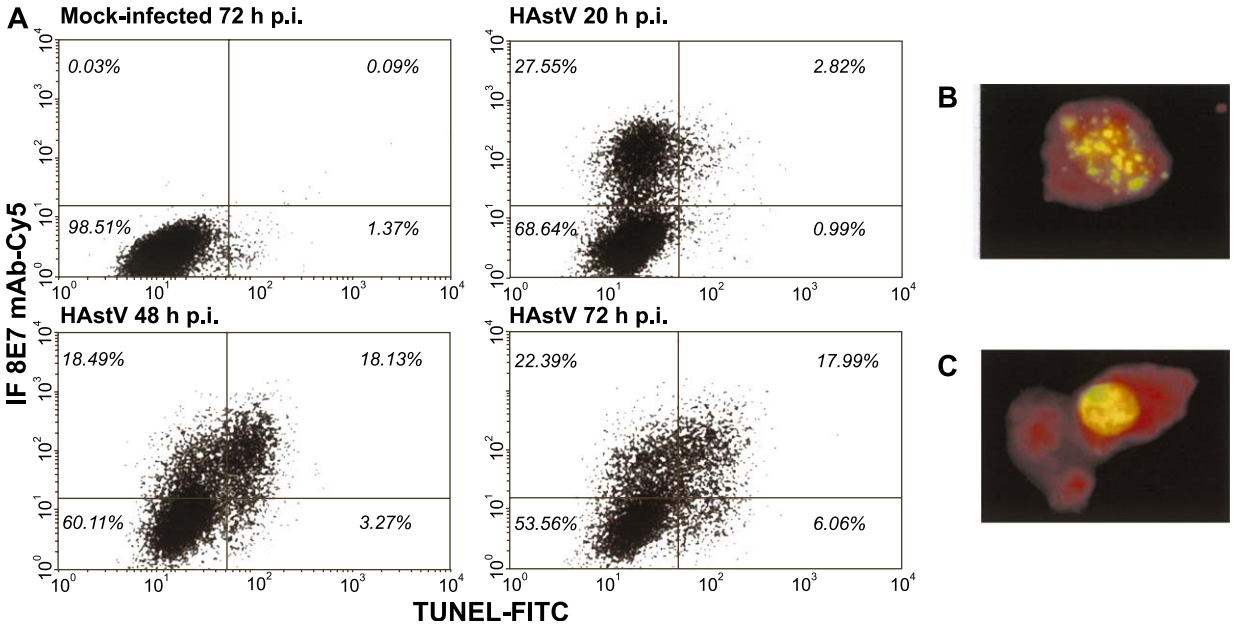

Fig. 6. Simultaneous determination of astrovirus antigens and apoptosis by flow cytometry. After apoptosis detection by TUNEL assay, an immunofluorescence analysis was performed on mock-infected and HAstV-infected CaCo-2 cells harvested at different times p.i. (A) Representative diagram of flow cytometry double labeling results. Cutoff values for positive cells were set so that more than 99.5% of total cells belonged to the lower left quadrant, in a dot plot of infected cells that had been labeled with negative control solution provided by the manufacturers for TUNEL and incubated with the cyanine5-conjugated anti-mouse antibody but not the astrovirus-specific monoclonal antibody (not shown). The total percentage of cells belonging to each quadrant is indicated. (B and C) Analysis of morphological changes of HAstV-infected cells at 72 h p.i. under a fluorescence microscope. Red color corresponds to the virus immunofluorescence, while green color corresponds to the FITC labeling of fragmented DNA due to apoptosis.

a lesser extent in non-infected cells, suggesting that the induction of apoptosis depends on active virus replication within the cell (Fig. 6A). At all times p.i., the proportion of TUNEL-labeled cells that expressed capsid proteins ranged between 74% and 84.7% and was three to five times higher than apoptotic cells that were negative for immunofluorescence. Notwithstanding, not all astrovirus-infected cells exhibited apoptotic features; both at 48 and 72 h p.i., approximately only 47.0% of antigen-positive cells were labeled with TUNEL. However, at an early time p.i., 20 h p.i., the subpopulation of apoptotic cells within the infected population represented only 9.3%, suggesting that viral replication within the cell occurs before the appearance of apoptosis.

Additionally, morphology of double-labeled cells was examined at 72 h p.i. under a fluorescence microscope. Since during apoptosis, genomic DNA breakage takes place at an earlier stage than nuclear fragmentation, not only cells with apoptotic bodies were positive by TUNEL (Fig. 6B), but also cells which showed clearly delimited nuclei (Fig. 6C).

To investigate the functional importance of apoptosis induction, the infectious titer of released virus was calculated. The effects of apoptosis on the replication of astrovirus were assayed by comparing virus production in the presence and absence of 100 μM Z-IETD-FMK and Z-LEHD-FMK at 48 h p.i. Viruses in the supernatant of infected cells were titrated using different approaches. Quantification of astrovirus progeny virions by both EIA and RT-PCR gave identical results in the absence or presence of any caspase inhibitors (Table 1). Infectious titers, obtained by an integrated cell culture RT-PCR procedure (Abad et al., 2001), were consistently higher than those measured by direct end-point RT-PCR titration. This is a consequence of the lower sensitivity of the end-point RT-PCR detection technique in comparison with the infectivity assay where an in vivo amplification in cell culture provides higher sensitivity. Surprisingly, inhibition of caspase 8 activity caused a 1-log-reduction in the infectious progeny. These results suggest a role of caspase 8-derived apoptosis in the astrovirus capsid maturation process that lead to infectious virion capsids.

Table 1
Effect of caspase inhibition on virus progeny release and infectivity[a]

	DMSO	Z-IETD-FMK	Z-LEHD-FMK
EIA[b]	10^3	10^3	10^3
RT-PCR[c]	10^5	10^5	10^5
Infectivity[d]	10^8	10^7	10^8

[a] Results are representative of two independent experiments (m.o.i. of 5), after incubation of 48 h p.i.
[b] Results are expressed as the reciprocal end-point dilution.
[c] Results are expressed as RT-PCR units per milliliter, after titration by end-point dilution RT-PCR.
[d] Results are expressed as infectious virus per milliliter and were measured by integrated cell culture RT-PCR procedure as previously described (Abad et al., 2001).

Induction of apoptosis by transient expression of ORF1a gene products in CaCo-2 cells

Recently, three related protein–protein interaction domains have been identified in molecules involved in apoptosis. They are known as the death domain superfamily, which includes death domains (DD), death effector domains (DED) and caspase recruitment domains (CARD). Each of the proteins belonging to this family interacts with other proteins through homotypic interactions and they are responsible for most of the specific recruitment events that take place during the apoptotic pathway. These domains possess remarkably similar structures consisting of six antiparallel α-helices with primarily hydrophobic core residues. The degree of similarity across the death domain superfamily can be rather low when measured by the amino acid sequence alignment alone without taking into consideration the structural information (Weber and Vincenz, 2001).

To screen for astrovirus encoded proapoptotic proteins, a computer analysis through the amino acid sequence of the three astrovirus ORFs was performed to identify potential domains related to apoptosis. Using the PredictProtein server, the analysis of the secondary structure of the whole astrovirus protein sequence revealed the presence of an optimal six α-helices structure of 95 amino acids close to the C terminus of ORF1a (from residue 620 to 714, accession number L23513). As a result of the proteolytical processing of ORF1a polyprotein suggested by Kiang and Matsui (2002), this region would be included in the putative nonstructural protein of unknown function p38. The average percentage of amino acid identity and similarity between this region and several members of the death domain superfamily were 19.1% and 41.7%, respectively. In addition, using the 3D-SSPM web server in search of 3D structural homologies, this region showed structural homology to the death domain found in human Fas (hFasDD). An alignment of all the available astrovirus sequences from this region and hFasDD is shown in Fig. 7. The presence of a death domain in a nonstructural protein of ORF1a suggests a direct link between this protein and the apoptotic pathway.

In this context, the ability of ORF1a to modulate apoptosis was examined by using a transient expression system. A plasmid containing the ORF1a (pcDNA1a) was transfected into CaCo-2 cells and a full-length ORF2 construct (pcDNA2) was included as a control. Upon electroporation of CaCo-2 cells, protein-expressing cells were labeled by immunofluorescence using antibodies against a synthetic peptide belonging to ORF1a and 8E7 monoclonal antibody for ORF2, while apoptotic nuclei were labeled by the TUNEL assay. Images of typical protein expressing cells are shown in Fig. 8. The percentage of protein-expressing cells that exhibited signs of apoptosis was calculated. The number of transfected cells that expressed viral proteins in each experiment was low,

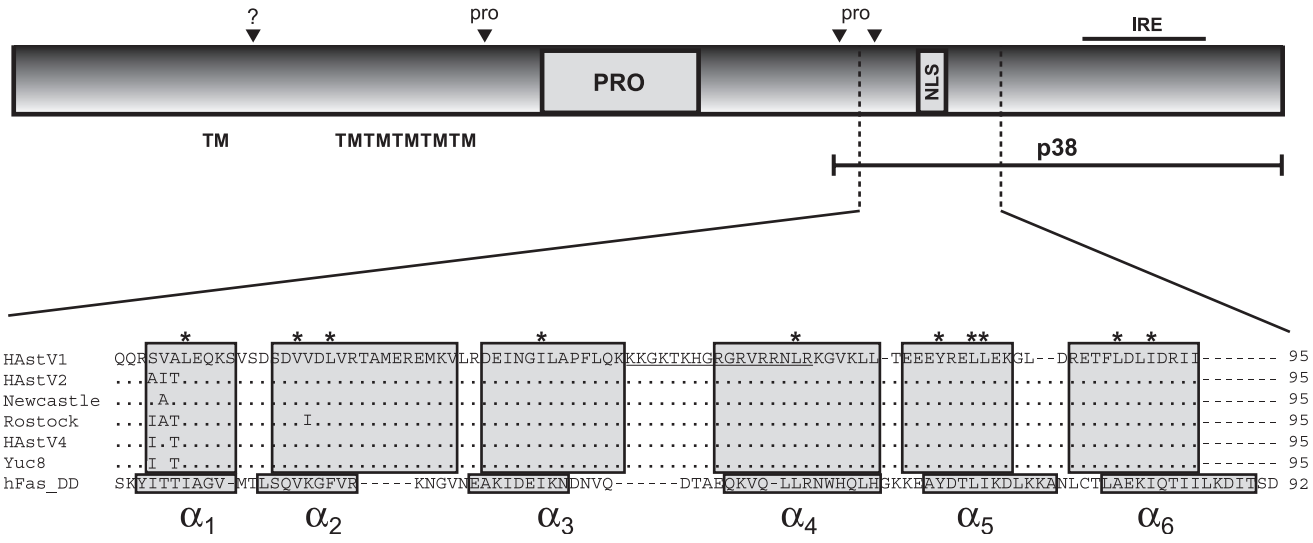

Fig. 7. Schematic diagram of astrovirus ORF1a. Predicted transmembrane helices (TM), protease motif (PRO), predicted nuclear localization signal (NLS) and an immunoreactive epitope (IRE) are shown. Black arrowheads refer to putative proteolytic cleavage sites, which seem to be dependent on both cellular proteases (?) and the viral protease (pro). The predicted death domain within ORF1a is indicated and a structure-based sequence alignment of all available HAstV sequences and the amino acid sequence of hFas death domain is shown. Helices are indicated by boxes and conserved hydrophobic core residues are indicated by an asterisk above the sequence. Underlined sequence corresponds to the NLS. Accession numbers L23513 (HAstV1), L13745 (HAstV2), Z25771 (A2/88 Newcastle), AF141381 (Rostock), AY257977 (HAstV4 p23795) and AF260508 (Yuc8).

reflecting the previously reported inefficiency of CaCo-2 cells transfection (Geigenmüller et al., 1997). However, a significantly higher number of apoptotic cells was observed after transfection of the ORF1a construct (27.3% ± 12.7%) than after transfection of the ORF2 construct (2.15% ± 2.15%), confirming the presence of a proapoptotic protein in ORF1a. Additionally, although an increase of the protein expression was observed with either construct up to 5 days p.i., a proportional increase in the percentage of apoptotic cells was only detected in the ORF1a-expressing cells.

Discussion

Mechanisms of virus-induced cell injury play an important role in the pathogenesis of viral infections. During the past few years, many efforts have been done to gain further insights into the virus–host cell interactions, and the number of viruses that have been shown to induce or inhibit apoptosis either directly or indirectly during their replication cycles has increased considerably (O'Brien, 1998). Although apoptotic cell death after virus infection has also been demonstrated for members of viral families taxonom-

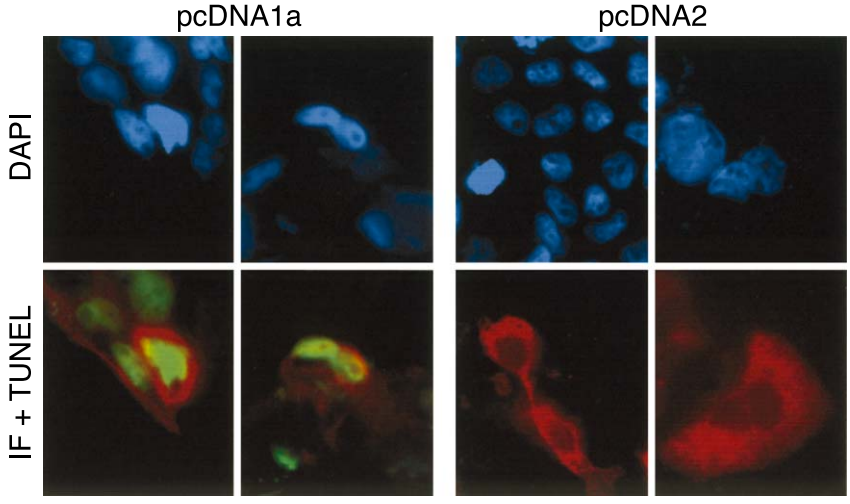

Fig. 8. Double labeling analysis of HAstV protein expression and apoptosis after transient expression of plasmids containing the full-length ORF1a and ORF2 constructs. Nuclei of all cells were counterstained with DAPI. Red color corresponds to immunofluorescence labeling and green color corresponds to apoptotic nuclei labeled by TUNEL.

ically not too distant to astrovirus, such as *Caliciviridae* and *Picornaviridae* (Al-Molawi et al., 2003; Alonso et al., 1998; Ammendolia et al., 1999; Kuo et al., 2002; López-Guerrero et al., 2000; Monroe et al., 1993), to our knowledge, this is the first report which provides evidence of an apoptotic response in human astrovirus-infected cells. Characteristic morphological and biochemical hallmarks of apoptosis, such as chromatin condensation, activation of cellular endonucleases, fragmentation of DNA and formation of apoptotic bodies, were detected in astrovirus-infected cells. There was a general agreement in results obtained with different techniques and apoptosis was induced in a dose-dependent pattern.

In the present report, activation of caspase 8 and caspase 9 was also explored to elucidate the underlying mechanisms of apoptosis induction. Caspases play a key role in the effector phase during apoptotic cell death and, while caspase 8 is an indicator of activation of the extrinsic apoptotic pathway, caspase 9 is an indicator of the mitochondrial apoptotic pathway. Notwithstanding, recent experiments have demonstrated that the hierarchy of caspase activation is not always maintained to promote the amplification of weaker apoptotic signals (Denecker et al., 2001; Kidd et al., 2000). It is now clear that in some types of cells, during the execution of the apoptotic extrinsic pathway, the death-inducing signaling complex (DISC) is not efficient enough to activate downstream effector caspases and therefore it requires amplification of the apoptotic signal by mitochondrial-mediated events. Caspase 8-mediated cleavage of a protein called Bid, which is a proapoptotic member of the Bcl-2 family, directs its translocation to the mitochondria, where it induces release of cytochrome *c* (Luo et al., 1998). Like in the cases of transmissible gastroenteritis coronavirus (Eleouet et al., 2000), Sendai virus (Bitzer et al., 2002), parvovirus B19 (Sol et al., 1999) or Langat flavivirus (Prikhod'ko et al., 2002), our results, both by Western blot and specific inhibition experiments, suggest that caspase 8 pathway is involved in the apoptotic response during astrovirus infection.

The viral gene product that is responsible for inducing apoptosis in RNA viruses has been characterized in several cases such as porcine reproductive and respiratory syndrome virus (Fernandez et al., 2002; Suarez et al., 1996), murine coronavirus (An et al., 1999), infectious bursal disease virus (Fernandez-Arias et al., 1997), HIV (Muthumani et al., 2002; Stewart et al., 2000), poliovirus (Barco et al., 2000; Goldstaub et al., 2000), influenza virus (Schultz-Cherry et al., 2001), Langat flavivirus (Prikhod'ko et al., 2002) or enterovirus 71 (Kuo et al., 2002). For other RNA virus such as Sindbis virus (Jan and Griffin, 1999) or reovirus (Connolly and Dermody, 2002), induction of apoptosis does not require virus replication. After transient expression experiments, our observations suggest that an apoptosis inducer may be encoded in ORF1a of astrovirus. Little is known about the biological function of the nonstructural proteins of astrovirus ORF1a, except that they contain a 3C-like serine protease motif (Matsui and Greenberg, 2001). In addition, a nuclear localization signal (NLS) has also been detected (Jiang et al., 1993) and astrovirus nonstructural proteins have been found in the nuclei of infected cells (Willcocks et al., 1999). The biological significance of this nuclear involvement in astrovirus life cycle is not fully understood. ORF1a and ORF1b are encoded in two separate reading frames, but are believed to be translated as a polyprotein. None of the proteolytic cleavage sites that are present within ORF1a have been fully characterized by N-terminal sequencing of the processed products. Between the protease motif and the nuclear localization signal, two different cleavage sites have been proposed using different approaches (Geigenmüller et al., 2002a, 2002b; Kiang and Matsui, 2002). By computer analysis, we have identified a potential death domain motif within the nonstructural protein p38 of astrovirus, based on the proteolytic model proposed by Kiang and Matsui (2002). The prediction of coiled-coils regions close to the C terminus of ORF1a have also been recently reported in both human and animal astrovirus by Jonassen et al. (2003). Death domains are one form of the prototypical protein-interacting domains that play important roles in many of the protein–protein interactions that take place both during the initial and the effector phases of apoptosis. A great degree of amino acid conservation is observed among the human astrovirus serotypes which have been sequenced at this region. The presence of a death domain would bring useful information on the role of this nonstructural protein. Further characterization of the p38 nonstructural protein in virus-infected cells and mutagenesis studies of its proapoptotic domain are under way.

Nevertheless, in both astrovirus-infected cells and transient ORF1a-expressing cells, not all cells were apoptotic. Only when using a high m.o.i. and long times p.i., around 70% of cells underwent apoptosis. Several reasons could explain why not all astrovirus-infected cells undergo apoptosis. One possibility could result from a technical problem, causing that the apoptotic stage of some infected cells would not be detectable by the TUNEL method. Another explanation could be that at a given time p.i., due to different stages of the virus replication cycle, the amount of apoptosis-inducing viral protein produced within some cells would be still too low to induce apoptosis. Even a viral apoptotic inhibitor could also be encoded in a different part of the genome. An intricate balance between both viral and cellular proapoptotic and antiapoptotic stimuli within the cell may decide whether it will die by apoptosis or not. In cell differentiating types such as CaCo-2 cells, this balance may be even more variable depending on the stage of differentiation.

Interestingly, in the presence of a caspase 8 specific inhibitor, there was a significant reduction in the infectivity of the virus progeny, while the titer of physical virions (estimated by EIA and RT-PCR) was not affected. These data are different from those obtained for other viruses such as Sendai virus (Bitzer et al., 1999), transmissible gastroenteritis coronavirus (Eleouet et al., 1999) or avian coronavirus

infectious bronchitis virus (Liu et al., 2001), whose virus production was not reduced when inhibiting the apoptotic process. From our results, we conclude that apoptotic death of host cells seems necessary for efficient astrovirus particle maturation. For some viruses, it has been observed that some of their proteins undergo caspase-mediated proteolysis within the host cell (Al-Molawi et al., 2003; Eleouet et al., 2000; Zhirnov et al., 1999). The astrovirus capsid processing and assembly is still controversial. Recently, different models have been proposed by different authors using different human astrovirus serotypes (Bass and Qiu, 2000; Geigenmüller et al., 2002a, 2002b; Méndez et al., 2002), and the action of a cellular protease has been suggested. Sequence analysis of all the available human amino acid sequences of ORF2 reveals the presence of some putative caspase cleavage sites close to the C terminus of the polyprotein. The relationship between a potential role of caspase-dependent capsid maturation and the physiological significance of apoptosis induction by human astrovirus in intestinal cells is currently being investigated.

Materials and methods

Cells and virus

The human colon adenocarcinoma cell line CaCo-2 was used throughout this work. Cells were grown in Eagle's minimum essential medium (MEM) supplemented with 10% fetal bovine serum. A tissue culture-adapted strain of human astrovirus serotype 4 (p23795), kindly provided by W.D. Cubitt from the Great Ormond Street Hospital for Children, London, was propagated in CaCo-2 cells, as previously described (Pintó et al., 1994). However, in the apoptosis studies, no trypsin was added to the p.i. medium to ensure a single cycle of virus replication (Bass and Qiu, 2000; Méndez et al., 2002; Monroe et al., 1991). Briefly, 3-day-old cell monolayers were washed twice with phosphate-buffered saline (PBS) and inoculated with viral stocks pretreated with 10 μg/ml trypsin (GIX Sigma) for 30 min at 37 °C. After a 1-h adsorption at 37 °C, MEM supplemented with 2% FBS was added. As apoptotic cells usually round up and detach from the surface of the culture flask, a mixed population of both suspended and attached cells was always used. At different times p.i., floating cells were harvested and pooled with the attached cells, which were recovered by trypsin treatment. Supernatant fluids of uninfected CaCo-2 cell lysates were used for mock infections.

Apoptosis inducing agent

A 0.5 M aspirin stock solution (ASA: acetylsalicylic acid; kindly provided by Bayer AG) in 0.75 M Tris–HCl (pH 7.4) was prepared. To induce apoptosis, CaCo-2 cell monolayers were washed twice with PBS and incubated for 48 h at 37 °C with MEM 2% FBS containing 15 mM aspirin (Ricchi et al., 1997). Tris–HCl buffer without aspirin was included in all experiments as negative control for aspirin-induced apoptosis.

Observation of nuclear morphology

Morphology of the infected cell nuclei was examined after fixation of cells for 30 min with 3% paraformaldehyde in PBS. Cells were stained with 1 μg/ml DAPI (Roche) in PBS for 20 min, washed twice with PBS, coverslipped and observed under a fluorescence microscope (Leica DMRB FLUO). The procedure was performed at room temperature.

Analysis of cellular DNA content

A previously described procedure (Gong et al., 1994) for DNA extraction from apoptotic cells was used with minor modifications to detect the reduction in DNA content within apoptotic cells (sub-G_0/G_1 DNA peak technique). Briefly, 2×10^6 cells were washed in PBS and fixed overnight at −20 °C, in 70% ice-cold ethanol. Cell pellets were resuspended in 40 μl of phosphate–citrate buffer, consisting of 192 parts of 0.2 M Na_2HPO_4 and 8 parts of 0.1 M citric acid (pH 7.8), at 37 °C for 30 min. After centrifugation at 1000 × g for 5 min, the cell pellet was resuspended in 1 ml of PBS containing 15 μg/ml propidium iodide (Molecular Probes), 0.1% Triton X-100 and 2 μg/ml DNase-free RNAse from bovine pancreas (Roche). After 1 h at room temperature, around 7000–10,000 cells were analyzed by flow cytometry (Immunotech Coulter XL).

Terminal deoxynucleotidyl transferase-mediated dUTP nick end labeling (TUNEL) assay

DNA fragmentation, which occurs within apoptotic cells, was also studied using the In Situ Cell Detection Kit, Fluorescein (Roche), following the manufacturer's instructions. Briefly, 2×10^6 cells were fixed in 3% paraformaldehyde in PBS and permeabilized with 0.1% Triton X-100 and 0.1% sodium citrate in PBS. DNA strand breaks were labeled at 3′OH ends by the addition of fluorescein dUTP using a terminal deoxynucleotidyl transferase (TdT). Cells were analyzed by flow cytometry (Immunotech Coulter XL) and also by optic microscopy (Leica DMRB FLUO) after performing a DAPI staining, as previously described.

Electron microscopy

For transmission electron microscopy studies, mock-infected and astrovirus-infected cells grown on 100-mm plates were washed twice with PBS, fixed with 3% paraformaldehyde and 2.5% glutaraldehyde in cacodylate buffer (pH 7.4) for 2 h at 4 °C, and harvested by scraping. Detached cells were collected and mixed with the suspension of adherent cells after performing the same fixation procedure. After low-speed centrifugation, cell pellets were

washed five times for 1 h at 4 °C with 0.1 M sodium cacodylate buffer (pH 7.4), post fixed with 1% osmium tetroxide in 0.1 M sodium cacodylate buffer for 1 h 30 min at room temperature, dehydrated in acetone series, and embedded in Spurr resin. Ultrathin sections were stained in uranylacetate and lead citrate and observed under an electron microscope (Hitachi HT-600).

Analysis of caspase 8 activation by Western blot

Cell lysates were prepared from 2×10^6 infected or mock-infected cells in 0.2 ml of RIPA buffer (50 mM Tris–HCl pH 7.8, 150 mM NaCl, 1% Nonidet NP-40, 0.1% SDS). Protein concentrations were calculated using the following formula: Protein concentration (mg/ml) = $(1.55 \times A_{280}) - (0.76 \times A_{260})$. Protein concentrations were standardized among samples and confirmed by Coomassie blue staining. After 12% SDS-polyacrylamide gel electrophoresis, proteins were electroblotted onto nitrocellulose membranes (Schleicher & Schuell). Membranes were blocked overnight at 4 °C in 5% skim milk powder in TBS buffer (10 mM Tris–HCl and 150 mM NaCl, pH 7.5), and an anti-caspase 8 rabbit polyclonal antibody (Pharmingen) was applied diluted 1:1000 for 3 h at room temperature. An alkaline phosphatase-conjugated anti-rabbit antibody (Sigma) was used as detecting antibody and X-Phosphate and NBT (Roche) were used as substrates.

Analysis of cytochrome c subcellular localization

At designated times p.i., around 7×10^6 cells were collected and resuspended in 1 ml of ice-cold buffer A (10 mM HEPES, 250 mM sucrose, 1 mM EGTA, pH 7.4). Cells were kept for 15 min on ice and homogenized using a syringe and centrifuged for 10 min at $1000 \times g$ to remove unlysed cells and nuclei. The supernatant fluids were transferred to new tubes and centrifuged again at $10{,}000 \times g$ for 20 min. Supernatant fluids from the second centrifugation represent the cytosolic fractions, whereas the pellets, resuspended in 50 μl of buffer A, represent mitochondrial fractions. The presence of cytochrome *c* was analyzed by Western blot as described above, using a dilution 1:100 of purified mouse anti-cytochrome *c* monoclonal antibody (Pharmingen), and an alkaline phosphatase-conjugated anti-mouse antibody (Pharmingen) as a secondary antibody. As before, protein concentration were standardized to produce comparable data. As positive controls, CaCo-2 cells were incubated with staurosporine (Sigma) at 1 μM final concentration for 24 h.

Inhibition of apoptosis

After infecting 1×10^6 cells, caspase specific peptides inhibitors Z-IETD-FMK and Z-LEHD-FMK (Sigma) were resuspended in dimethyl sulfoxide (DMSO) and added to the overlay medium at 10, 100 and 150 μM concentration. An equivalent volume of DMSO was added to a control of infection lacking caspase inhibitors. Percentages of apoptotic cells were measured by flow cytometry after performing the TUNEL assay at 48 h p.i.

Double labeling of cells for detection of apoptosis and viral antigens

Around 2×10^6 infected or mock-infected cells were fixed in 3% paraformaldehyde in PBS for 30 min at room temperature and permeabilized in PBS with 0.1% Triton X-100 and 0.1% sodium citrate for 10 min on ice. After washing three times with PBS, cells were blocked for 30 min at room temperature in PBS containing 3% BSA (Sigma) and 0.1% Tween 20. For viral antigen detection, an immunofluorescence analysis using the anti-astrovirus monoclonal antibody 8E7 diluted 1:10,000 (kindly provided by J. Herrmann) was performed. At this point, samples were divided in two aliquots and incubated with different secondary anti-mouse antibodies (Amersham Pharmacia Biotech): cyanine5-conjugated antibody at a dilution of 1:100, and cyanine3-conjugated antibody at a dilution of 1:5000. All antibodies were diluted in 3% BSA–0.1% Tween 20 in PBS and incubations performed for 1 h at room temperature. After immunofluorescence labeling, cells were washed twice in PBS, prior performing the TUNEL assay as described above. Cyanine5-labeled cells were analyzed by flow cytometry (Immunotech Coulter XL) and cyanine3-labeled cells were analyzed under a fluorescence microscope (Leica DMRB FLUO).

Effects of caspase inhibitors on virus production

Virus production in the supernatant medium of infected cells (released virus) at 48 h p.i. in the presence or absence of 100 μM caspase inhibitors (Z-IETD-FMK and Z-LEHD-FMK) was evaluated by three different methods. First, the amount of astrovirus antigen in dilutions of the supernatant medium was measured by indirect enzyme immunoassay as described by Herrmann et al. (1990). Second, the titer of astrovirus genomes was measured by end-point dilution RT-PCR, using primers A1 and A2, as previously described (Guix et al., 2002; Willcocks et al., 1994). Finally, infectious titer was measured by a previously described method (Abad et al., 2001). Briefly, samples were pretreated with trypsin and 10-fold dilutions were inoculated onto CaCo-2 cells monolayers grown in 24-well plates. Trypsin was added to the p.i. medium and the presence of virus in the supernatant of each dilution was evaluated by RT-PCR using primers A1 and A2, after 6 days of incubation.

Computer sequence analysis

Secondary structure was predicted using the PredictProtein server (http://www.embl-heidelberg.de/predictprotein/predictprotein.html). Protein fold recognition using 1D and 3D sequence profiles coupled with secondary structure and

solvation potential information was studied using the web server 3D-PSSM V2.6.0 (Kelley et al., 2000).

Construction of plasmids

Complete astrovirus ORF1a and ORF2 were cloned into pcDNA3.1(+) mammalian expression vector (Invitrogen). Fragments containing the full-length ORF1a (nucleotides 79–2884 from Genbank accession number L23513) and ORF2 (nucleotides 4317–6691 from Genbank accession number L23513) were generated by PCR amplification using plasmid pAVIC6 kindly provided by Dr. Suzanne Matsui (Geigenmüller et al., 1997). Sequence of the primers containing *Not*I and *Xho*I restriction sites are 5′ATAGCGGCCG CAACAAGATGGCA3′ and 5′TCCCTCGAG CTAATGAGTGGTAA3′ for ORF1a, and 5′AGGGCGGCCG CAAAGAAGTGTGATG3′ and 5′CCCCTCGAG CTACT CGGCGTGGC3′ for ORF2 (the underlining indicates the restriction site introduced in each primer). Recombinant pcDNA3.1(+) plasmids pcDNA1a and pcDNA2 were constructed by cloning the restricted PCR fragments into *Not*I- and *Xho*I-digested pcDNA3.1(+).

Transient expression assays for apoptosis

Recombinant constructs pcDNA1a and pcDNA2, and plasmid pcDNA3.1 without insert, were introduced into CaCo-2 cells by electroporation in a BTX Electro Cell Manipulator 600, using a cuvette gap of 0.2 cm and a final volume of 0.5 ml. Subconfluent CaCo-2 cell monolayers were trypsinized and washed in HeBS buffer (20 mM Hepes, 137 mM NaCl, 5 mM KCl, 0.7 mM Na_2HPO_4, 6 mM Dextrose; pH 7.05). Approximately 1×10^6 cells were electroporated with 280 V and a capacitance of 500 μF in the presence of 200 μg of plasmid; two pulses were used. Cells were diluted into growth medium and seeded into 24-well plates containing glass coverslips. At 72 h posttransfection, cells were fixed and analyzed by double labeling under a fluorescence microscope. Protein expression of ORF1a was detected by immunofluorescence using a mouse antibody made against a synthetic peptide corresponding to amino acid residues 778–792 of ORF1a (Genbank accession number L23513). For ORF2 expression, mouse monoclonal antibody 8E7 was used. Apoptosis was measured by performing the TUNEL assay and nuclei of all cells were counterstained with DAPI. The percentage of transfected cells that exhibited apoptotic nuclei was estimated after counting 50–100 protein-expressing cells from each condition and analyzing their nuclei. The same experiment was repeated twice for each construct.

Acknowledgments

S. Guix was recipient of a FI fellowship from the Generalitat de Catalunya. We acknowledge the technical expertise of the Serveis Científic-Tècnics of the University of Barcelona. We are grateful to J. Calbó, T. Mampel, A. Mazo and M. Zamora, from the Department of Biochemistry and Molecular Biology of the University of Barcelona for useful discussion and advice. This work was supported in part by grants QLRT-1999-0594 from the European Union, and 1997/SGR/00224 and 2001/SGR/00098 from the Generalitat de Catalunya.

References

Abad, F.X., Villena, C., Guix, S., Caballero, S., Pintó, R.M., Bosch, A., 2001. Potential role of fomites in the vehicular transmission of human astroviruses. Appl. Environ. Microbiol. 37, 3904–3907.

Al-Molawi, N., Beardmore, V.A., Carter, M.J., Kass, G.E.N., Roberts, L.O., 2003. Caspase-mediated cleavage of the feline calicivirus capsid protein. J. Gen. Virol. 84, 1237–1244.

Alonso, C., Oviedo, J.M., Martin-Alonso, J.M., Diaz, E., Boga, J.A., Parra, F., 1998. Programmed cell death in the pathogenesis of rabbit hemorrhagic disease. Arch. Virol. 143, 321–332.

Ammendolia, M.G., Tinari, A., Calcabrini, A., Superti, F., 1999. Poliovirus infection induces apoptosis in CaCo-2 cells. J. Med. Virol. 59, 122–129.

An, S., Chen, C., Yu, X., Leibowitz, J.L., Makino, S., 1999. Induction of apoptosis in murine coronavirus-infected cultured cells and demonstration of E protein as an apoptosis inducer. J. Virol. 73, 7853–7859.

Barco, A., Feduchi, E., Carrasco, L., 2000. Poliovirus protease 3Cpro kills cells by apoptosis. Virology 266, 352–360.

Bass, D.M., Qiu, S., 2000. Proteolytic processing of the astrovirus capsid. J. Virol. 74, 1810–1814.

Bitzer, M., Armeanu, S., Prinz, F., Ungerechts, G., Wybranietz, W., Spiegel, M., Bernlöhr, C., Cecconi, F., Gregor, M., Neubert, W.J., Schulze-Osthoff, K., Lauer, U.M., 2002. Caspase-8 and Apaf-1-independent caspase-9 activation in Sendai virus-infected cells. J. Biol. Chem. 277, 29817–29824.

Bitzer, M., Prinz, F., Bauer, M., Spiegel, M., Neubert, W.J., Gregor, M., Schulze-Osthoff, K., Lauer, U., 1999. Sendai virus infection induces apoptosis through activation of caspase-8 (FLICE) and caspase 3 (CPP32). J. Virol. 73, 702–708.

Connolly, J.L., Dermody, T.S., 2002. Virion disassembly is required for apoptosis induced by reovirus. J. Virol. 76, 1632–1641.

Denecker, G., Vercammen, D., Declercq, W., Vandenabeele, P., 2001. Apoptotic and necrotic cell death induced by death domain receptors. Cell. Mol. Life Sci. 58, 356–370.

Eleouet, J.-F., Chilmonczyk, S., Besnardeau, L., Laude, H., 1999. Transmissible gastroenteritis coronavirus induces programmed cell death in infected cells through a caspase-dependent pathway. J. Virol. 72, 4918–4924.

Eleouet, J.-F., Slee, E.A., Saurini, F., Castagne, N., Poncet, D., Garrido, C., Solary, E., Martin, S.J., 2000. The viral nucleocapsid protein of transmissible gastroenteritis coronavirus (TGEV) is cleaved by caspase-6 and -7 during TGEV-induced apoptosis. J. Virol. 74, 3975–3983.

Fernandez, A., Suarez, P., Castro, J.M., Tabares, E., Diaz-Guerra, M., 2002. Characterization of regions in the GP5 protein of porcine reproductive and respiratory syndrome virus required to induce apoptotic cell death. Virus Res. 83, 103–118.

Fernandez-Arias, A., Martinez, S., Rodriguez, J.F., 1997. The major antigenic protein of infectious bursal disease virus, VP2, is an apoptotic inducer. J. Virol. 71, 8014–8018.

Geigenmüller, U., Ginzton, N.H., Matsui, S.M., 1997. Construction of a genome-length cDNA clone for human astrovirus serotype 1 and synthesis of infectious RNA transcripts. J. Virol. 71, 1713–1717.

Geigenmüller, U., Chew, T., Ginzton, N., Matsui, S.M., 2002a. Processing of nonstructural protein 1a of human astrovirus. J. Virol. 76, 2003–2008.

Geigenmüller, U., Ginzton, N.H., Matsui, S.M., 2002b. Studies on intracellular processing of the capsid protein of human astrovirus serotype 1 in infected cells. J. Gen. Virol. 83, 1691–1695.

Glass, R.I., Noel, J., Mitchell, D.K., Herrmann, J.E., Blacklow, N.R., Pickering, L.K., Dennehy, P., Ruiz-Palacios, G., de Guerrero, M.L, Monroe, S.S., 1996. The changing epidemiology of astrovirus-associated gastroenteritis: a review. Arch. Virol. 12, 287–300 (Supplement).

Goldstaub, D., Grady, A., Berkovich, Z., Grossmann, Z., Nophar, Y., Luria, S., Sonenberg, N., Kahana, C., 2000. Poliovirus 2A protease induces apoptotic cell death. Mol. Cell. Biol. 20, 1271–1277.

Gong, J., Traganos, F., Darzynkiewicz, Z., 1994. A selective procedure for DNA extraction from apoptotic cells applicable for gel electrophoresis and flow cytometry. Anal. Biochem. 218, 314–319.

Gray, E.W., Angus, K.W., Snodgrass, D.R., 1980. Ultrastructure of the small intestine in astrovirus-infected lambs. J. Gen. Virol. 49, 71–82.

Guix, S.S., Caballero, S., Villena, C., Bartolomé, R., Latorre, C., Rabella, N., Simó, M., Bosch, A., Pintó, R.M., 2002. Molecular epidemiology of astrovirus infection in Barcelona, Spain. J. Clin. Microbiol. 40, 133–139.

Hardwick, J.M., 1998. Viral interference with apoptosis. Cell Dev. Biol. 9, 339–349.

Herrmann, J.E., Hudson, R.W., Perron-Henry, D.M., Kurtz, J.B., Blacklow, N.R., 1988. Antigenic characterization of cell-cultivated astrovirus serotypes and development of astrovirus-specific monoclonal antibodies. J. Infect. Dis. 158, 182–185.

Herrmann, J.E., Nowak, N.A., Perron-Henry, D.M., Hudson, R.W., Cubitt, W.D., Blacklow, N.R., 1990. Diagnosis of astrovirus gastroenteritis by antigen detection with monoclonal antibodies. J. Infect. Dis. 161, 226–229.

Jan, J.-T., Griffin, D.E., 1999. Induction of apoptosis by Sindbis Virus occurs at cell entry and does not require virus replication. J. Virol. 73, 10296–10302.

Jiang, B., Monroe, S.S., Koonin, E.V., Stine, S.E., Glass, R.I., 1993. RNA sequence of astrovirus: distinctive genomic organization and a putative retrovirus-like ribosomal frameshifting signal that directs the viral replicase synthesis. Proc. Natl. Acad. Sci. U.S.A. 90, 10539–10543.

Jonassen, C.M., Jonassen, T.O., Sveen, T.M., Grinde, B., 2003. Complete genomic sequences of astroviruses from sheep and turkey: comparison with related viruses. Virus Res. 91, 195–201.

Kelley, L.A., MacCallum, R.M., Sternberg, M.J.E., 2000. Enhanced genome annotation using structural profiles in the program 3D-PSSM. J. Mol. Biol. 299, 499–520.

Kiang, D., Matsui, S.M., 2002. Proteolytic processing of a human astrovirus nonstructural protein. J. Gen. Virol. 83, 25–34.

Kidd, V.J., Lahti, J.M., Teitz, T., 2000. Proteolytic regulation of apoptosis. Cell Dev. Biol. 11, 191–201.

Koyama, A.H., Fukumori, T., Fujita, M., Irie, H., Adachi, A., 2000. Physiological significance of apoptosis in animal virus infection. Microbes Infect. 2, 1111–1117.

Kuo, R.L., Kung, S.H., Hsu, Y.Y., Liu, W.T., 2002. Infection with enterovirus 71 or expression of its 2A protease induces apoptotic cell death. J. Gen. Virol. 83, 1367–1376.

Liu, C., Xu, H.Y., Liu, D.X., 2001. Induction of caspase-dependent apoptosis in cultured cells in the avian coronavirus infectious bronchitis virus. J. Virol. 75, 6402–6409.

López-Guerrero, J.A., Alonso, M., Martín-Belmonte, F., Carrasco, L., 2000. Poliovirus induces apoptosis in the human U937 promonocytic cell line. Virology 272, 250–256.

Luo, X., Budihardjo, I., Zou, H., Slaughter, C., Wang, X., 1998. Bid, a Bcl-2 interacting protein, mediates cytochrome *c* release from mitochondria in response to activation of cell surface death receptors. Cell 94, 481–490.

Matsui, S.M., Greenberg, H.B., 2001. Astroviruses. In: Fields, B.N., Knipe, D.M., Howley, P.M., Griffin, D.E., Martin, M.A., Lamb, R.A., Roizman, B., Straus, S.E. (Eds.), Fields Virology. Lippincott Williams & Wilkins, Philadelphia, PA, pp. 875–893.

Medema, J.P., Scaffidi, C., Kischkel, F.C., Shevchenko, A., Mann, M., Krammer, P.H., Peter, M.E., 1997. FLICE is activated by association with the CD95 death-inducing signaling complex (DISC). EMBO J. 16, 2794–2804.

Méndez, E., Fernández-Luna, T., López, S., Méndez-Toss, M., Arias, C. 2002. Proteolytic processing of a serotype 8 human astrovirus ORF2 polyprotein. J. Virol. 76, 7996–8002.

Monroe, S.S., Stine, S.E., Gorelkin, L., Herrmann, J.E., Blacklow, N.R., Glass, R.I., 1991. Temporal synthesis of proteins and RNAs during human astrovirus infection in cultured cells. J. Virol. 65, 641–648.

Monroe, S.S., Jiang, B., Stine, S.S., Koopmans, M., Glass, R.I., 1993. Subgenomic RNA sequence of human astrovirus supports classification of Astroviridae as a new family of RNA viruses. J. Virol. 67, 3611–3614.

Muthumani, K., Hwang, D.S., Desai, B.M., Zhang, D., Dayes, N., Green, D.R., Weiner, D.B., 2002. HIV-1 Vpr induces apoptosis through caspase 9 in T cells and peripheral blood mononuclear cells. J. Biol. Chem. 277, 37820–37831.

O'Brien, V., 1998. Viruses and apoptosis. J. Gen. Virol. 79, 1833–1845.

Pintó, R.M., Díez, J.M., Bosch, A., 1994. Use of the colonic carcinoma cell line CaCo-2 for in vivo amplification and detection of enteric viruses. J. Med. Virol. 44, 310–315.

Prikhod'ko, G.G., Prikhod'ko, E.A., Pletnev, A.G., Cohen, J.I., 2002. Langat flavivirus protease NS3 binds caspase-8 and induces apoptosis. J. Virol. 76, 5701–5710.

Qureshi, M.A., Saif, Y.M., Heggen-Peay, C.L., Edens, F.W., Havenstein, G.B., 2001. Induction of functional defects in macrophages by poult enteritis and mortality syndrome-associated turkey astrovirus. Avian Dis. 45, 853–861.

Ricchi, P., Pignata, S., Di Popolo, A., Memoli, A., Apicella, A., Zarrilli, R., Acquaviva, A.M., 1997. Effect of aspirin on cell proliferation and differentiation of colon adenocarcinoma Caco-2 cells. Int. J. Cancer 73, 880–884.

Roulston, A., Marcellus, R.C., Branton, P.E., 1999. Viruses and apoptosis. Annu. Rev. Microbiol. 53, 577–628.

Saraste, A., Pulkki, K., 2000. Morphologic and biochemical hallmarks of apoptosis. Cardiovasc. Res. 45, 528–537.

Schultz-Cherry, S., Dybdahl-Sissoko, N., Neuman, G., Kawaoka, Y., Hinshaw, V.S., 2001. Influenza virus NS1 induces apoptosis in cultured cells. J. Virol. 75, 7875–7881.

Sol, N., Le Junter, J., Vassias, I., Freyssinier, J.M., Thomas, A., Prigent, A.F., Rudkin, B.B., Fichelson, S., Morinet, F., 1999. Possible interactions between the NS-1 protein and tumor necrosis factor alpha pathways in erythroid cell apoptosis induced by human parvovirus B19. J. Virol. 73, 8762–8770.

Stennicke, H.R., Salvesen, G.S., 2000. Caspases-controlling intracellular signals by protease zymogen activation. Biochim. Biophys. Acta 1477, 299–306.

Stewart, S.A., Poon, B., Song, J.Y., Chen, I.S.Y., 2000. Human immunodeficiency virus type 1 Vpr induces apoptosis through caspase activation. J. Virol. 74, 3105–3111.

Suarez, P., Diaz-Guerra, M., Prieto, C., Esteban, M., Castro, J.M., Nieto, A., Ortin, J., 1996. Open reading frame 5 of porcine reproductive respiratory syndrome virus as a cause of virus-induced apoptosis. J. Virol. 70, 2876–2882.

Thome, M., Schneider, P., Hofmann, K., Fickenscher, H., Meinl, E., Neipel, F., Mattmann, C., Bujrns, K., Bodmer, J.-L., Schroter, M., Scaffidi, C., Krammer, P.H., Peter, M.E., Tschopp, J., 1997. Viral FLICE-inhibitory proteins (FLIPs) prevent apoptosis induced by death receptors. Nature 386, 517–521.

Thornberry, N.A., Rano, T.A., Peterson, E.P., Rasper, D.M., Timkey, T., Garcia-Calvo, M., Houtzager, V.M., Nordstrom, P.A., Roy, S., Vaillancourt, J.P., Chapman, K.T., Nicholson, D.W., 1997. A combinatorial approach defines specificities of members of the caspase family and granzyme B. J. Biol. Chem. 272, 17907–17911.

Weber, C.H., Vincenz, C., 2001. The death domain superfamily: a tale of two interfaces? Trends Biochem. Sci. 26, 475–481.

Willcocks, M.M., Ashton, N., Kurtz, J.B., Cubitt, W.D., Carter, M.J., 1994. Cell culture adaptation of astrovirus involves a deletion. J. Virol. 68, 6057–6058.

Willcocks, M.M., Boxal, A.S., Carter, M.J., 1999. Processing and intracellular location of human astrovirus non-structural proteins. J. Gen. Virol. 80, 2607–2611.

Woode, G.N., Pohlenz, J.F., Kelso Gourley, N.E., Fagerland, J.A., 1984. Astrovirus and breda virus infections of dome cell epithelium of bovine ileum. J. Clin. Microbiol. 19, 623–630.

Zhirnov, O.P., Konakova, T.E., Garten, W., Klenk, H.D., 1999. Caspase-dependent N-terminal cleavage of influenza virus nucleocapsid protein in infected cells. J. Virol. 73, 10158–10163.